J Mol Model (2015) 21: 260
DOI 10.1007/s00894-015-2802-2

ORIGINAL PAPER

DFT studies on the palladium-catalyzed dearomatization reaction between naphthalene allyl chloride and allyltributylstannane

Wei Cao [1] · **Dongxu Tian** [1] · **Dongxue Han** [1]

Received: 14 April 2015 / Accepted: 26 August 2015 / Published online: 16 September 2015

Abstract The Pd-catalyzed dearomatization of naphthalene allyl chloride with allyltributylstannane has been investigated using density functional theory (DFT) calculations at the B3LYP level. The calculations indicate that the (η^1-allyl)(η^3-allyl)Pd(PH_3) complex is responsible for the formation of *ortho*-dearomatized product. Moreover it is easy to produce the *ortho*-dearomatized product when reductive elimination starts from (η^3-allylnaphthalene)(η^1-allyl)Pd complex 7, while it is easy to form the *para*-dearomatized product when reductive elimination starts from (η^3-allylnaphthalene)(η^1-allyl)Pd complex 9. The Stille coupling products can't be produced due to high reaction energy barrier.

Keywords Dearomatization · DFT · NBO · Propenylnaphthalene

Introduction

The alicyclic complexes frequently appear in the molecules of natural products and bioactive compounds. Therefore the synthesis of alicyclic compounds has received considerable interest in recent years. Aromatic compounds are stable and widely available. Thus it is an important method to synthesize alicyclic complexes by dearomatization reaction [1–7]. However, the dearomatization of arenes is especially difficult because the delocalization of π bonds makes aromatic compounds very stable. Over the past few decades, many methods have been developed to accomplish the dearomatization reaction, such as electrophilic addition [8], nucleophilic addition [9, 10], photocycloaddition [11], and so on [12]. Remarkably, the transition-metal-mediated dearomatization methodology has been an efficient method, due to the complexation of aromatic system to transition metals that leads to the activation of arenes and facilitates the electrophilic addition of [M(η^2-arene)] (M= Os, Re, Mo, and W) complexes and the nucleophilic addition of [M(η^6-arene)] (M=Cr, Mn, and Ru) complexes [13].

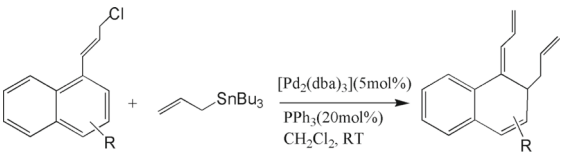

(1)

Recently, Bao and co-workers [14] reported the dearomatization reaction of naphthalene allyl chloride with allyltributylstannane in the presence of Pd catalyst, which is displayed in Eq. (1). The *ortho*-dearomatized product, not the *para*-dearomatized and Stille cross-coupling products, is synthesized. Meanwhile, they proposed a plausible mechanism (Scheme 1). In the past few years, there have been many DFT studies on mechanisms of similar reactions. For example, Ariafard and co-workers [15] studied the Pd-catalyzed *para*-dearomatization reaction of benzyl chloride with allyltributylstannane. Ren and co-workers [16] reported the Pd-catalyzed dearomatization of naphthalene allyl chloride with allenyltributylstannane, which also produce the *ortho*-dearomatized product. Then Ren and co-workers [17] investigated a theoretical study on the mechanism of palladium-catalyzed *para*-dearomatization

✉ Dongxu Tian
tiandx@dlut.edu.cn

[1] State Key Laboratory of Fine Chemicals, Dalian University of Technology, Dalian 116024, China

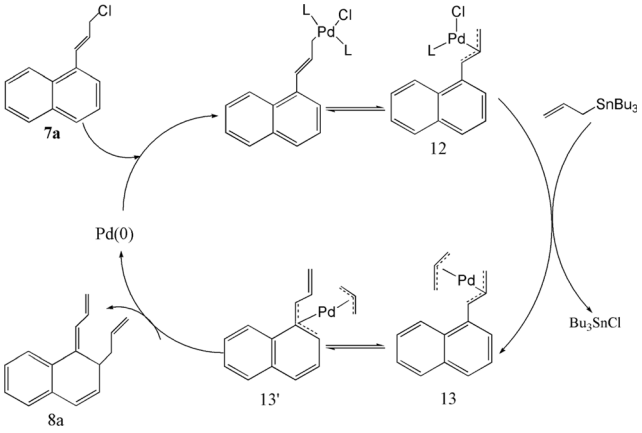

Scheme 1 The mechanism proposed by Bao and co-workers

of chloromethylnaphthalene with allenyltributylstannane. However, no theoretical study has been reported about the *ortho*-dearomatization of naphthalene allyl chloride with allyltributylstannane in the presence of Pd catalyst. Therefore many details are lacking for the reaction mechnism. For example, what are the structures of transition states? Why does this reaction form *ortho*-dearomatized product, not *para*-dearomatized product? Why does this reaction not give Stille cross-coupling product?

To answer the questions raised above and provide insight into portions of this unusual reaction, we have studied the Pd-catalyzed dearomatization of naphthalene allyl chloride with allyltributylstannane using the B3LYP density functional theory. We investigate the mechanism proposed by Bao, in which the main intermediates are bis(η^3-ally)palladium complexes. Then a different mechanism is calculated, in which the main intermediates are (η^1-allyl)(η^3-allyl)Pd(PH_3) complexes. In addition to the *ortho*-dearomatized product, the pathways to generate the *para*-dearomatized and Stille cross-coupling products are also examined.

Computational details

All calculations in this study are performed with Guassian03 suite of programs [18]. The geometries of the reactants, transition states, intermediates, and products are fully optimized without any symmetry constraints at the B3LYP level [19–21] of density functional theory (DFT). Frequencies are computed at the same level of theory for all the stationary points to characterize the transition states (one imaginary frequency) and the equilibrium structures (no imaginary frequency). The effective core potentials of Hay and Wadt with double-ξ, valance basis sets (LanL2DZ) [22, 23] are used for Pd, Sn, and P; the standard polarized 6-31G(d) basis set is chosen to describe C and Cl; and H is described by 6-31G basis set [24, 25]. Polarization functions are added for Sn(ξ,d=0.183), C(ξ,d=0.8), P(ξ,d=0.34), and Cl(ξ,d=0.514) [26]. Calculations of intrinsic reaction coordinates (IRC) [27, 28] are performed on transition states to confirm that such structures are indeed connecting two minima. Natural charges and electron occupancy are analyzed with natural bond orbital (NBO) [29]. The triphenylphosphine ligand PPh_3 is modeled by PH_3, the geometry around the metal center in each of the structures is only a little different from the structures that were calculated with the triphenylphosphine [15, 16].

Scheme 2 Mechanism 1

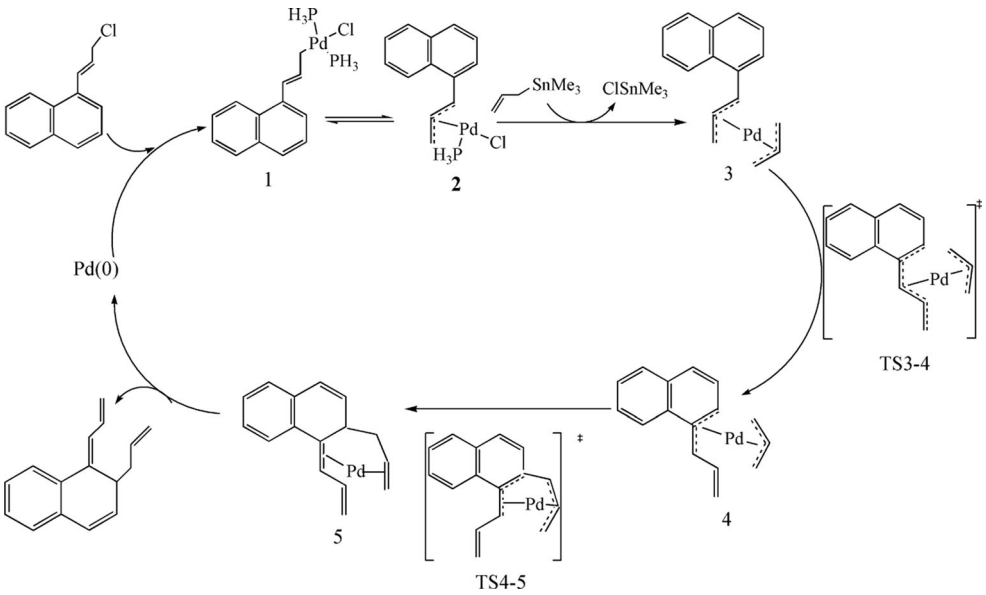

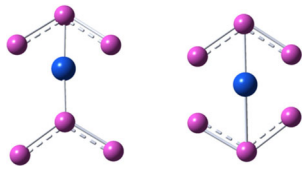

Scheme 3 *cis*-structure (left) and *trans*-structure (right)

Results and discussion

Dearomatization reaction mechanisms

Two kinds of dearomatization reaction mechanisms for *ortho*-dearomatized products are examined. As shown in Scheme 2, the main intermediates are bis(η^3-ally)palladium complexes in mechanism 1 reported by Bao and co-workers [14]. In Scheme 4, the main intermediates are (η^1-allyl)(η^3-allyl)palladium complexes in mechanism 2.

As shown in mechanism 1(Scheme 2), the (η^3-ally)(η^3-allylnaphthalene)palladium intermediate 3 isomerizes to (η^3-ally)(η^3-allylnaphthalene)palladium complex 4 via TS3-4 that completes the rearrangement of bis(η^3-ally)palladium complex. Reductive elimination step starts from intermediate 4 by directly coupling the C of η^3-ally ligand with the ortho carbon of the η^3-allylnaphthalene ligand via TS4-5.

In mechanism 1, because the coordination mode of intermediate 3 is bis(η^3-ally)palladium, the pathway includes the *cis*-structure and *trans*-structure pathways starting from intermediate 3. The *cis*-structure and *trans*-structure are shown in Scheme 3. Figure 1 shows the energy profiles of the *cis*-structure and *trans*-structure pathways. As shown in Fig. 1, the *trans*-intermediates (3*trans*, 4*trans*, and 5*trans*) are more stable than the *cis*-intermediates (3*cis*, 4*cis*, and 5*cis*). However, the *cis*-transition states have relatively lower energy than the *trans*-transition states. The energy barriers of *cis*-structure pathway and *trans*-structure pathway are 44.28 and 53.73 kcal mol^{-1}, respectively. The *cis*-structure pathway is more favorable kinetically than *trans*-structure pathway. Therefore, mechanism 1 is not feasible kinetically because of a relatively large energy barrier.

Because of the relatively large energy barrier in mechanism 1, mechanism 2 is proposed as shown in Scheme 4. The (η^1-allylnaphthalene)(η^3-allyl)Pd(PH_3) intermediate 6 isomerizes to (η^3-allylnaphthalene)(η^1-allyl)Pd(PH_3) intermediate 7 via TS6-7 that completes the rearrangement of (η^1-allyl)(η^3-allyl)Pd(PH_3) complex. Reductive elimination step starts from intermediate 7 by directly coupling terminal carbon of the η^1-ally ligand with the ortho carbon of η^3-allylnaphthalene ligand via TS7-8.

In mechanism 2, because the coordination mode of TS6-7 is bis(η^3-ally)palladium, the pathway includes the *cis*-structure and *trans*-structure pathways starting from TS6-7. As shown in Fig. 2, the energy barriers of the *cis*-structure and *trans*-structure pathways are 18.68 and 24.21 kcal mol^{-1}, respectively. The *cis*-structure pathway is more favorable kinetically than *trans*-structure pathway. Compared to mechanism 1, the energy barriers of mechanism 2 are lower by respective 25.60 (*cis*-structure pathway) and 29.52 (*trans*-structure pathways) kcal mol^{-1}. Therefore mechanism 2 is more favorable kinetically.

Ren and co-workers [16] reported the Pd-catalyzed dearomatization of naphthalene allyl chloride with allenyltributylstannane, which is displayed in Eq. (2). The difference from the present study is taking allenyltributylstannane as the reagent in place of allyltributylstannane. Two kinds of

Scheme 4 Mechanism 2

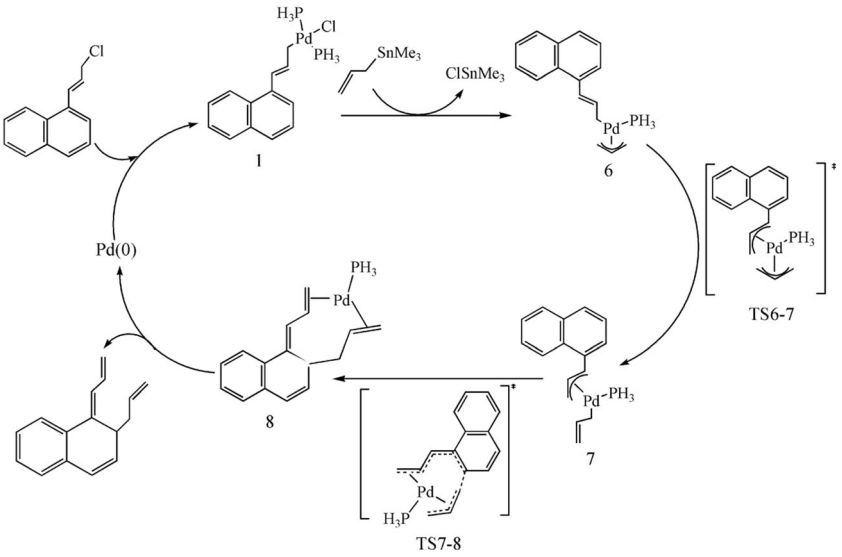

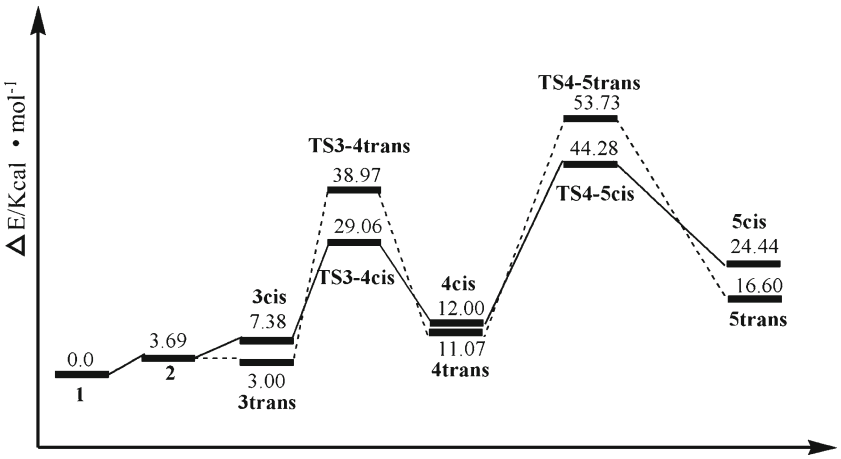

Fig. 1 Relative energy profiles for mechanism 1 (dotted and solid lines are the *trans*-structure and *cis*-structure pathways, respectively)

dearomatization reactions in the reductive elimination are compared in Scheme 5.

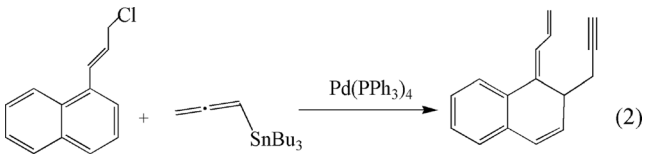

As shown in Scheme 5, the intermediates have the same coordination mode in the reductive elimination. Moreover, both of the η^1-ligands have an available electron pair to attack the ortho carbon of η^3-allylnaphthalene ligand via the transition states to form the dearomatization product. For the allyl ligand (Scheme 5a), the reductive elimination takes place from (η^1-allylnaphthalene)(η^3- allyl)Pd(PH_3) intermediate 6. Then the intermediate 6 isomerizes to (η^3-allylnaphthalene)(η^1-allyl)Pd(PH_3) intermediate 7. The dearomatization product is formed by directly coupling terminal carbon of the η^1-ally ligand with the ortho carbon of η^3-allylnaphthalene ligand via TS7-8. For the allenyl ligand (Scheme 5b), the reductive elimination takes place from (η^1-allylnaphthalene)(η^3-propargyl)Pd(PH_3) intermediate 15. Then the intermediate 15 isomerizes to (η^3-allylnaphthalene)(η^1-allenyl)Pd(PH_3) intermediate 16. The dearomatization product is formed by directly coupling the terminal carbon of the η^1-allenyl ligand with ortho carbon of the η^3-naphthalene ligand via TS16-17.

Structure analysis

The optimized structural parameters of transition states and intermediates in mechanism 1 and mechanism 2 are shown in Fig. 3. During the rearrangement of bis(η^3-ally)palladium complex in mechanism 1, the Pd-C5, Pd-C6, and Pd-C7 bonds in TS3-4 are 2.88, 2.11, and 3.07 Å. During the rearrangement of (η^1-allyl)(η^3-allyl)Pd(PH_3) complex in mechanism 2, the Pd-C4, Pd-C5, and Pd-C6 bonds in TS6-7 are 2.21, 2.19, and 2.40 Å. Therefore there is a stronger Pd- η^3-allylnaphthalene bond interaction in TS6-7 than in TS3-4. During the reductive elimination, there is a larger conjugated π system in TS7-8 than TS4-5.

The stability of transition states of mechanism 1 and 2 are investigated by NBO method. The NBO charge of TS3-4, TS4-5, TS6-7, and TS7-8 are summarized in Table 1. In TS3-4 and TS6-7, the positive charges of Pd are respectively

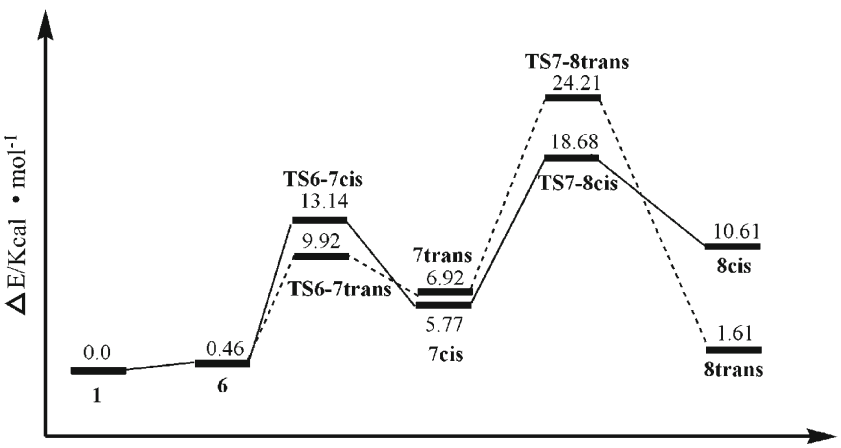

Fig. 2 Relative energy profiles for mechanism 2. (dotted and solid lines are the *trans*-structure and *cis*-structure pathways, respectively)

Scheme 5 Comparison of allyl (a) and allenyl (b) ligands in the reductive elimination

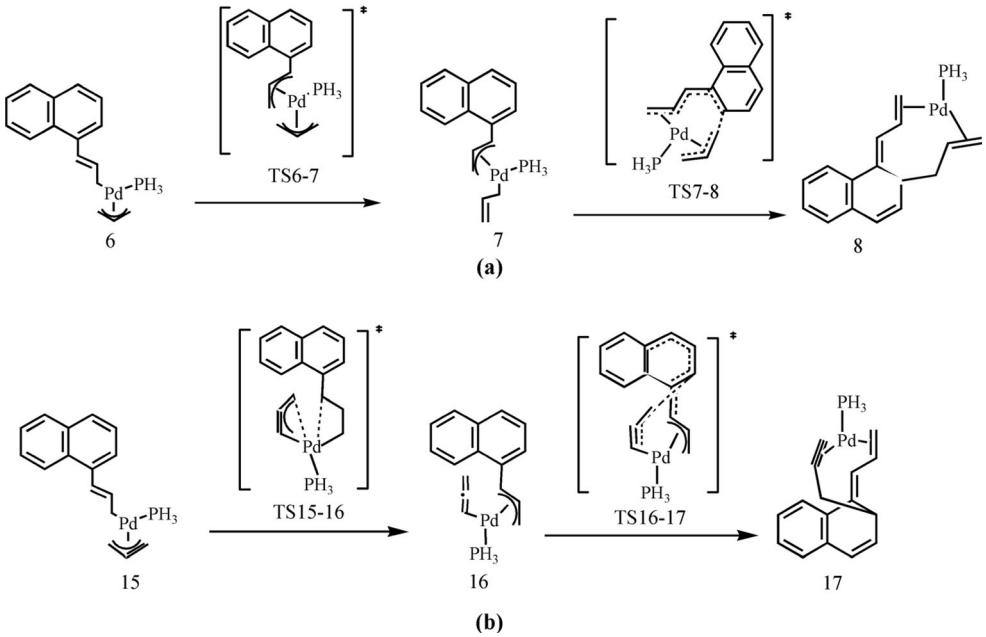

0.447e and 0.517e, while the negative charges of the sum of C1-C8 are −2.729e and −2.909e, respectively. In TS4-5 and TS7-8, the positive charges of Pd are respectively 0.248e and 0.325e, while the negative charges of the sum of C1-C8 are −2.558e and −2.808e, respectively. There is more electron transfer from Pd to coordinated C atoms in TS6-7 and TS7-8 than in TS3-4 and TS4-5. Furthermore, in reductive elimination, PH_3 donates an electron to Pd in mechanism 2.

The orbital occupancies of 5s and 4d of Pd in TS3-4, 4, TS4-5, TS6-7, 7, and TS7-8 are listed in Table 2. The orbital occupancies of 4d orbital of Pd in TS3-4 (9.232e) and in TS4-5 (9.433e) are larger than the ones in TS6-7 (9.219e) and TS7-8 (9.359), respectively. The orbital occupancies of 5s and 4d of Pd are consistent with the previous charge analysis of Pd in TS3-4, TS4-5, TS6-7, and TS7-8.

As shown in Table 2, from intermediate 7 to TS7-8, the orbital occupancies of 5s orbital decrease from 0.358e to 0.305e, while the orbital occupancies of 4d orbital increase from 9.243e to 9.359e. In TS7-8, the electrons transfer from the π orbital of allyl to 4d orbital of Pd, with the backdonation from 5s orbital of Pd to π* orbital of allyl. Therefore, the backdonation interaction makes the TS7-8 more stable. From

Fig. 3 Optimized structural parameters of transition states in mechanism 1 and mechanism 2 (bond lengths are in Å)

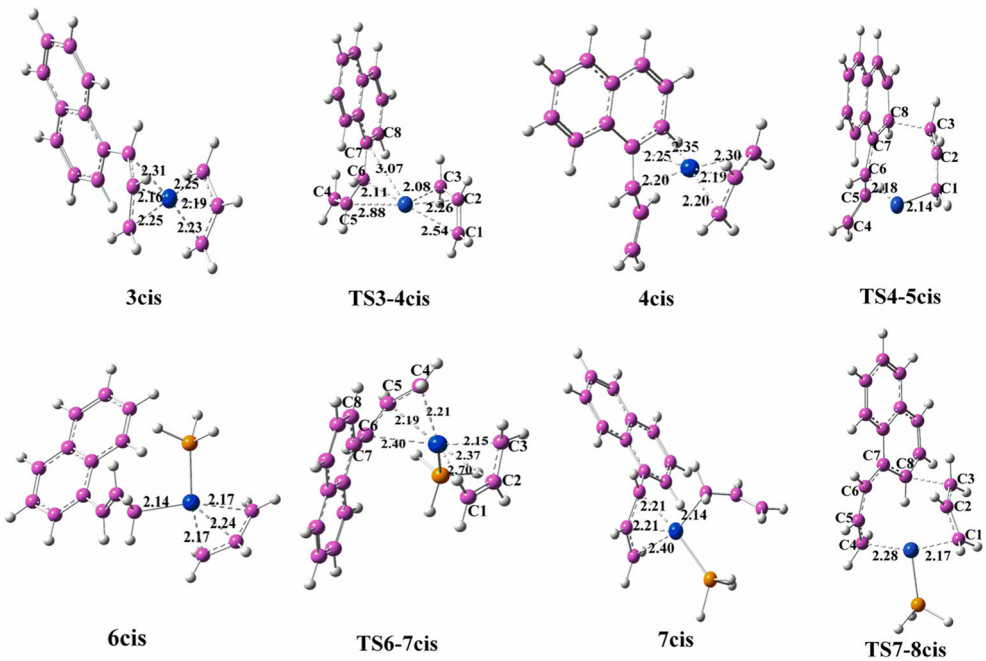

Table 1 NBO charge of transition states in mechanism 1 and mechanism 2

	TS3-4cis	TS4-5cis	TS6-7cis	TS7-8cis
Pd	0.447	0.248	0.517	0.325
C1	−0.529	−0.578	−0.637	−0.603
C2	−0.290	−0.224	−0.293	−0.334
C3	−0.492	−0.461	−0.482	−0.426
C4	−0.448	−0.426	−0.583	−0.618
C5	−0.242	−0.245	−0.290	−0.298
C6	−0.470	−0.345	−0.358	−0.244
C7	−0.014	−0.021	−0.041	−0.050
C8	−0.244	−0.258	−0.225	−0.235
ΣC	−2.729	−2.558	−2.909	−2.808
P	–	–	0.046	0.163

the geometric and electronic properties, TS6-7 and TS7-8 are more stable than TS3-4 and TS 4–5, respectively. Thus mechanism 2 is more favorable than mechanism 1.

Possible pathway to *para*-dearomatized product

The possible pathway to generate *para*-dearomatized product is studied. As displayed in Scheme 2, the process from 7 to 8 via TS7-8 is a crucial step for determining the dearomatized product. Therefore we start the calculation from intermediate 7. Firstly, intermediate 7 isomerizes to 9 that the Pd coordinates to the naphthalene ring, forming (η^3-allylnaphthalene)(η^1-allyl)Pd(PH_3) intermediate 9, which is shown in Fig. 4. Comparing intermediate 7 (in Fig. 2) and intermediate 9 (in Fig. 4), the intermediate *cis*-7 and *trans*-7 are more stable than 9 by 5.30 and 4.15 kcal mol^{-1}, respectively. Then intermediate 9 forms *para*-dearomatized product 10 via TS9-10, the overall barrier is 14.76 kcal mol^{-1}, which is 3.92 kcal mol^{-1} lower than the largest energy barrier in mechanism 2. Therefore *para*-dearomatization reaction is energetically feasible. It is easy to produce the *ortho*-dearomatized product when reductive elimination starts from (η^3-allylnaphthalene)(η^1-allyl)Pd(PH_3) intermediate 7. It is easy to form the *para*-dearomatized product when reductive

Table 2 The orbital occupancies of Pd in mechanism 1 and 2

Pd	5s	$4d_{xy}$	$4d_{xz}$	$4d_{yz}$	$4d_{x^2y^2}$	$4d_{z^2}$	Σ4d
TS3-4cis	0.318	1.853	1.936	1.823	1.931	1.689	9.232
4cis	0.253	1.868	1.835	1.914	1.735	1.841	9.193
TS4-5cis	0.264	1.904	1.884	1.910	1.925	1.810	9.433
TS6-7cis	0.238	1.973	1.711	1.885	1.787	1.863	9.219
7cis	0.358	1.928	1.906	1.787	1.726	1.896	9.243
TS7-8cis	0.305	1.928	1.899	1.802	1.864	1.866	9.359

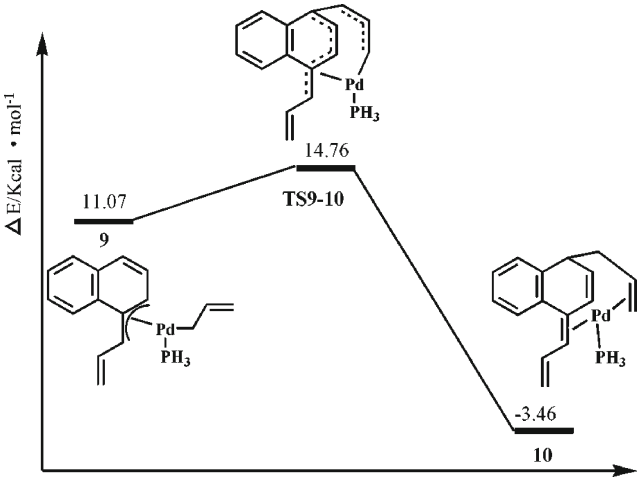

Fig. 4 Relative energy profiles for the possible dearomatization product from intermediate 9

elimination starts from (η^3-allylnaphthalene)(η^1-allyl)Pd(PH_3) intermediate 9.

Possible pathway to Stille coupling product

The reaction is possible to generate Stille coupling products, which are expected products of organic electrophiles (RX) with organostannanes(R′SnR″$_3$) [30]. The pathways directly coupling the allyl and the propenylnaphthalene groups are calculated from the intermediates 3 *cis* and 6. Figure 5 shows the energy profiles calculated for two direct coupling pathways. The energy barriers of two pathways are calculated to be 42.43 (TS_{3-11}) and 22.44(TS_{6-14}) kcal mol^{-1}, respectively. The energy barriers of direct coupling are higher than the energy barrier of dearomatization (18.68 kcal mol^{-1}). Consistent with the experimental observation, the dearomatized product is produced in palladium-catalyzed dearomatization reaction of propenylnaphthalene chlorine with allyltributylstannane.

Conclusions

The palladium-catalyzed dearomatization reaction of propenylnaphthalene chlorine with allyltributylstannane has been studied using density functional theory calculations at the B3LYP level. Our calculation shows the energy barrier of mechanism 1 is 44.28 kcal mol^{-1} (*trans*-structure pathway is 53.73 kcal mol^{-1}), which is unfavorable kinetically. The energy barrier of mechanism 2 is 18.68 kcal mol^{-1} (*trans*-structure pathway is 24.21 kcal mol^{-1}). Therefore this *ortho*-dearomatization reaction proceeds by mechanism 2, in which (η^1, η^3-allyl) palladium complexes are the main intermediates and reductive elimination starts from (η^3-allylnaphthalene)(η^1-allyl)Pd(PH_3) intermediate 7. By the analysis of geometry, NBO charge and orbital occupancies of 5s and 4d of Pd, the

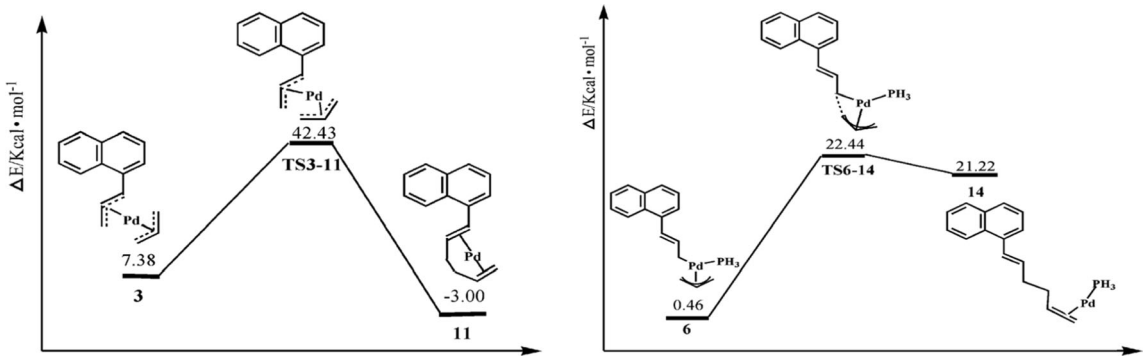

Fig. 5 Relative energy profiles calculated for the possible Stille coupling product from intermediate 3 *cis* (*left*) and 6 (*right*)

transition states in mechanism 2 are more stable than transition states in mechanism 2. Moreover the *cis*-structure pathway is more favorable than *trans*-structure pathway. The pathway to *para*-dearomatization product is examined from (η^3-allylnaphthalene)(η^1-allyl)Pd(PH_3) intermediate 9. The energy barrier is only 14.76 kcal mol^{-1}. Thus the *para*-dearomatized product is easily formed when reductive elimination starts from (η^3-allyl naphthalene)(η^1-allyl)Pd(PH_3) intermediate 9. The possible Stille coupling products are also examined. The energy barriers of two pathways are calculated to be respectively 42.43 and 22.44 kcal mol^{-1}. Which are higher than the energy barrier of dearomatization reaction(18.68 kcal mol^{-1}). At last, we illustrate the similarity between allayl and allenyl ligands in the reductive elimination, in which the intermediates have the same coordination mode and both of the η^1-ligands have an available electron pair to interact with the ortho carbon.

Acknowledgments This work was supported by the National Science Foundation of China (21001019) the Fundamental Research Funds for the Central Universities (DUT15LK24). The results were obtained on the ScGrid of Supercomputing Center, Computer Network Information Center of Chinese Academy of Sciences.

References

1. Bao M, Nakamura H, Yamamoto Y (2001) J Am Chem Soc 123: 759–760
2. García-Fortanet J, Kessler F, Buchwald SL (2009) J Am Chem Soc 131:6676–6677
3. Lee S, Chataigner I, Piettre SR (2011) Angew Chem Int Ed 50:472–476
4. Peng B, Feng X, Zhang X, Zhang S, Bao M (2010) J Org Chem 75: 2619–2627
5. Pouységu L, Deffieux D, Quideau S (2010) Tetrahedron 66:2235–2261
6. Rousseaux S, García-Fortanet J, Del Aguila Sanchez MA, Buchwald SL (2011) J Am Chem Soc 133:9282–9285
7. Rudolph A, Bos PH, Meetsma A, Minnaard AJ, Feringa BL (2011) Angew Chem Int Ed 50:5834–5838
8. Delafuente DA, Myers WH, Sabat M, Harman WD (2005) Organometallics 24:1876–1885
9. Clayden J, Kenworthy MN, Helliwell M (2003) Org Lett 5:831–834
10. Zhou L, Wu LZ, Zhang LP, Tung CH (2006) Organometallics 25: 1707–1711
11. Kohmoto S, Masu H, Tatsuno C, Kishikawa K, Yamamoto M, Yamaguchi K (2000) J Chem Soc Perkin Trans 1:4464–4468
12. Boivin J, Yousfi M, Zard SZ (1997) Tetrahedron Lett 38:5985–5988
13. Pape AR, Kaliappan KP, Kündig EP (2000) Chem Rev 100:2917–2940
14. Lu S, Xu Z, Bao M, Yamamoto Y (2008) Angew Chem Int Ed 47: 4366–4369
15. Ariafard A, Lin Z (2006) J Am Chem Soc 128:13010–13016
16. Ren Y, Jia J, Zhang T, Wu H, Liu W (2012) Organometallics 31: 1168–1179
17. Ren Y, Jia J, Liu W, Wu H (2013) Organometallics 32:52–62
18. Frisch MJ, Trucks GW, Schlegel HB, Scuseria GE, Robb MA, Cheeseman JR, Montgomery JA, Vreven T Jr, Kudin KN, Burant JC, Millam JM, Iyengar SS, Tomasi J, Barone V, Mennucci B, Cossi M, Scalmani G, Rega N, Petersson GA, Nakatsuji H, Hada M, Ehara M, Toyota K, Fukuda R, Hasegawa J, Ishida M, Nakajima T, Honda Y, Kitao O, Nakai H, Klene M, Li X, Knox JE, Hratchian HP, Cross JB, Bakken V, Adamo C, Jaramillo J, Gomperts R, Stratmann RE, Yazyev O, Austin AJ, Cammi R, Pomelli C, Ochterski JW, Ayala PY, Morokuma K, Voth GA, Salvador P, Dannenberg JJ, Zakrzewski VG, Dapprich S, Daniels AD, Strain MC, Farkas O, Malick DK, Rabuck AD, Raghavachari K, Foresman JB, Ortiz JV, Cui Q, Baboul AG, Clifford S, Cioslowski J, Stefanov BB, Liu G, Liashenko A, Piskorz P, Komaromi I, Martin RL, Fox DJ, Keith T, Al-Laham MA, Peng CY, Nanayakkara A, Challacombe M, Gill PMW, Johnson B, Chen W, Wong MW, Gonzalez C, and Pople JA (2004) Gaussian Inc, Wallingford
19. Becke AD (1993) J Chem Phys 98:5648
20. Lee C, Yang W, Parr RG (1988) Phys Rev B 37:785–789
21. Miehlich B, Savin A, Stoll H, Preuss H (1989) Chem Phys Lett 157: 200–206
22. Hay PJ, Wadt WR (1985) J Chem Phys 82:270
23. Hay PJ, Wadt WR (1985) J Chem Phys 82:299
24. Davidson ER, Feller D (1986) Chem Rev 86:61–696
25. Hariharan PC, Pople JA (1973) Theor Chim Acta 28:213–222
26. Ehlers AW, Böhme M, Dapprich S, Gobbi A, Höllwarth A, Jonas V, Köhler KF, Stegmann R, Veldkamp A, Frenking G (1993) Chem Phys Lett 208:111–114
27. Fukui K (1970) J Chem Phys 74:4161–4163
28. Fukui K (1981) Acc Chem Res 14:363–368
29. Reed AE, Curtiss LA, Weinhold F (1988) Chem Rev 88:899–926
30. Milstein D, Stille JK (1979) J Am Chem Soc 101:4992–4998